Electronic structure of VO$_2$ studied by x-ray photoelectron and x-ray emission spectroscopies

E Z Kurmaev†, V M Cherkashenko†, Yu M Yarmoshenko†, St Bartkowski‡, A V Postnikov‡, M Neumann‡, L-C Duda§, J H Guo§, J Nordgren§, V A Perelyaev‖ and W Reichelt¶

† Institute of Metal Physics, Russian Academy of Sciences, Ural Division, Yekaterinburg GSP-170, Russia
‡ Universität Osnabrück, Fachbereich Physik, D-49069 Osnabrück, Germany
§ Physics Department, Uppsala University, Box 530, S-75121 Uppsala, Sweden
‖ Institute of Solid State Chemistry, Russian Academy of Sciences, Ural Division, Yekaterinburg GSP-145, Russia
¶ Technische Universität Dresden, Institut für Anorganische Chemie, Mommsenstrasse 13, D-01062 Dresden, Germany

Abstract. A VO$_2$ single crystal has been the subject of a combined investigation by high-resolution x-ray photoelectron spectroscopy (XPS), x-ray emission spectroscopy (XES) with both electron and energy-selective x-ray excitation (V Lα, V Kβ_5 and O Kα emission) and x-ray absorption spectroscopy (XAS) (O 1s). We performed first-principles tight-binding LMTO band-structure calculations for VO$_2$ in both the monoclinic and tetragonal rutile phases and compared the densities of states (DOS) with the experimental data. From this we conclude that the electronic structure of VO$_2$ is more bandlike than correlated.

1. Introduction

VO$_2$ belongs to the group of transition metal compounds which exhibit metal–insulator transitions [1]. At $T = 340$ K, VO$_2$ undergoes a phase transition from a semiconductor with monoclinic structure to a metal with the tetragonal rutile structure. The nature of the ground-state semiconducting phase is still rather uncertain. In the semiconducting phase, the V atoms are paired, which is why the suggestion was made that the electron–phonon interaction is responsible for the splitting of the d band and the opening of a band gap [2]. This idea is supported by band-structure calculations according to which the crystallographic phase transition can be explained by the formation of a charge-density wave accompanied by a lattice distortion and a subsequent condensation of phonons [3]. According to reference [4], there is enough energy gain to account for the metal–insulator transition through structural distortions that permits a strengthening of the vanadium d–d bonds and a reorganization of the states near the Fermi level.

On the other hand, some calculations indicate that a crystallographic distortion is not sufficient to open up a gap, and that the electron-correlation effects play an important role in the transition [5]. It was concluded in reference [6] that the energy gap in VO$_2$ is of the charge-transfer type rather than of the Mott–Hubbard type as in the late-transition-metal compounds, like NiO and CuO [7].

In addition to earlier spectroscopic studies [8–11], photoelectron spectroscopy measurements and low-energy electron diffraction studies on VO_2 have been carried out recently in references [12, 13]. The present work aims at a combined experimental study of the electronic structure of a VO_2 single crystal at room temperature by the use of high-energy spectroscopies. A high-resolution x-ray photoelectron spectroscopy (XPS) study provides information about the total density of states (DOS) in the valence band (VB); V Lα (the 3d4s $\rightarrow$ 2p transition), V Kβ_5 (the 4p $\rightarrow$ 1s transition), O Kα (the 2p $\rightarrow$ 1s transition) and x-ray emission (XES) VB spectra (excited by both electrons and photons) probe the V 3d, V 4p and O 2p partial DOS in the valence band; the O 1s total-electron-yield spectrum probes the O 2p unoccupied states. Band-structure calculations are performed and compared with the experimental spectra leading to the conclusion that the electronic structure of VO_2 is more bandlike than correlated.

2. Experimental procedure

The XPS measurements were carried out with a PHI 5600 ci multi-technique spectrometer using monochromatized aluminium Kα radiation with a full width at half-maximum (FWHM) of 0.3 eV. The energy resolution of the analyser was 1.5% of the pass energy. We estimate an energy resolution of about 0.35 eV for the XPS measurements on VO_2. The base pressure in the vacuum chamber during the measurements was 5×10^{-9} Torr. All of the experiments presented in this paper have been performed at room temperature with the same single crystal of VO_2 ($2 \times 7 \times 0.5$ mm).

The initial measurements were performed without cleaving the crystal, and hence a high contamination of carbon was detected on the surface. Therefore the final measurements were done on a surface that was cleaved *in vacuo*. Thus an excellent surface with a relatively small number of defects and contaminations could be obtained, and hence the intrinsic properties of the samples could be studied. For comparison, XPS measurements on pure V metal (single crystal) were also performed. All of the XPS spectra were calibrated using the Au 4f$_{7/2}$ signal from an Au foil ($E_{b.e.}(4f_{7/2}) = 84.0$ eV).

The electron-excited V Lα emission spectra (the 3d4s $\rightarrow$ 2p$_{3/2}$ transition) of VO_2 were recorded using an RSM-500 spectrometer with a diffraction grating ($N = 600$ lines mm^{-1}; $R = 6$ m). The accelerating voltage and current on the x-ray tube were $V = 4.4$ keV and $I = 0.3$ mA. The energy resolution was 0.4 eV.

The V Kβ_5 spectra (the 4p $\rightarrow$ 1s transition) of VO_2 were measured using a fluorescent Johan-type vacuum spectrometer with a position-sensitive detector [14]. Cu Kα x-ray radiation from the sealed x-ray tube was used for excitation for the fluorescent V Kβ_5 XES. A quartz crystal (rhombohedral plane, second-order reflection) curved to $R = 1.8$ m was used as an analyser. The spectra were measured with an energy resolution $\Delta E = 0.22$ eV.

The energy-selective excited O Kα (the 2p $\rightarrow$ 1s transition) and V Lα spectra (the 3d4s $\rightarrow$ 2p$_{3/2}$ transition) were measured as well as x-ray absorption spectra (the V 2p and O 1s edges) in the sample drain-current mode. These measurements were performed at the undulator beam line BW3 at HASYLAB Hamburg, Germany [15], equipped with a modified SX-700 monochromator. The soft-x-ray emission spectra were recorded at various excitation energies in the first order of diffraction with a resolution of about 0.7 eV. We used a grazing-incidence grating spectrometer [16] with an $R = 5$ m spherical grating with 1200 lines mm^{-1} in a Rowland circle geometry. The resolution of the excitation radiation was set to about 1 eV by opening the exit slit of the monochromator to 400 μm. The spectrometer had a solid-angle acceptance of about 2×10^{-5} sr, so with a spot size of some

500×500 μm at a distance of 5 cm from the entrance slit of the spectrometer we registered a maximum of about 300 counts min^{-1} in the V Lα line at 100 mA ring current. In order to obtain a reasonable statistical accuracy, we had to acquire data for 120 to 240 minutes per spectrum, according to the excitation energy. The angle between the incident x-ray beam and the detection direction was 90°. This minimized the elastic scattering into the spectrometer, because the polarization of the beam coincided with the detection direction. The V 2p and O 1s absorption spectra had energy resolutions of 0.2 eV for an exit slit width of 80 μm. No special surface preparation was undertaken for these measurements.
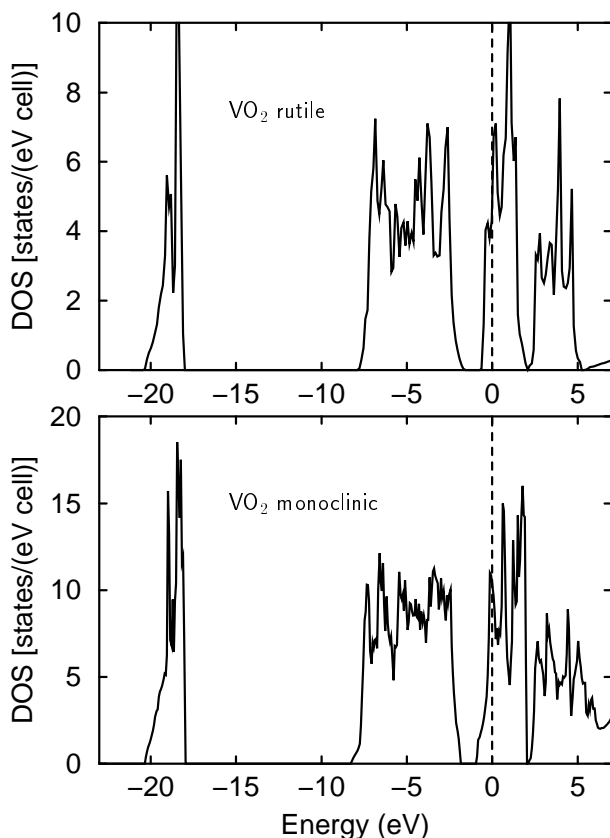

Figure 1. The total density of states calculated for the rutile (tetragonal) and monoclinic crystal structures of VO$_2$.

3. Results and discussion

3.1. Electronic structure calculations

The band-structure calculations were carried out by the tight-binding linear muffin-tin orbital method (TB-LMTO) in the atomic sphere approximation (ASA) [17], with the use of the exchange–correlation potential as parametrized by von Barth and Hedin [18] and gradient corrections as proposed by Langreth and Mehl [19] on top of the local density approximation (LDA). Since both the rutile and the monoclinic structures of VO$_2$ are relatively loosely packed, it was necessary to include empty spheres in the ASA calculations. For the

tetragonal rutile phase, we used the crystal structure parameters $a = 4.5546$ Å, $c/a = 0.626$ and $u = 0.300$ as given in reference [20]. Besides two formula units of VO_2, our unit cell included eight equivalent empty spheres, which form long chains parallel to the linear O–V–O fragments, separating the latter. Due to the difference between the V and O atomic sphere radii, the chains are slightly bent. Our choice of the sphere radii S, based on the attainability of good matching between the potential at the V and O atomic spheres compatible with a radial sphere overlap below 25% of all interatomic distances, was: $S(V) = 2.702$ au; $S(O) = 1.762$ au; S(empty spheres) $= 1.619$ au. The calculated band structure and the total DOS are fairly close to those obtained earlier in reference [3, 21, 22] by different methods. We performed our own calculation because no data on the partial DOS, which are necessary for the discussion of the XES, were available from the previous calculations. Our calculated total DOS for the rutile phase of VO_2 is shown in figure 1, upper panel.

As is usual in oxides, the valence band is formed by hybridized transition metal 3d and O 2p states. The band gap of 0.9 eV within the valence band separates the regions where O 2p states (below the gap) and V 3d states (above the gap) dominate. The Fermi level crosses the upper subband, revealing a metallic behaviour of VO_2, as is consistent with the results of other calculations done for the rutile-type structure [3, 4, 21, 22]. The O 2s-related subband (which experiences some hybridization with the V 3d and V 4p states) lies separately at about 20 eV below the Fermi level. The overall shape of the band structure and of the total DOS obtained in our calculation is in agreement with earlier results [3, 21, 22]; the width of the gap within the valence band is somewhat larger than 0.62 eV as obtained in the full-potential linear augmented-plane-wave calculation of reference [22]. The gap width of 4.6 eV reported in reference [3] seems to be too large (probably due to the use of the Slater exchange potential) and not in agreement with the experimental positioning of individual subbands, as discussed in reference [21] or found in the present paper.

Since the room-temperature phase (for $T < 68$ °C) of VO_2 is monoclinic, the relevant comparison with experiment needs the calculation data for the latter structure. The mono-clinic unit cell contains four formula units of VO_2, and, because of the large number of atoms and low symmetry, only few calculations have been done up to now. An earlier non-self-consistent calculation [23] reproduces an experimentally observable semiconductor band gap, but otherwise seems to be very inaccurate in its description of the overall structure of the valence band. The analysis of the structure transformation by means of *ab initio* molecular dynamics in reference [4] shows that the monoclinic phase has lower energy than the rutile phase, and the equilibrium positions of the atoms are in good agreement with the experimental determination. However, the strength of the tendency to open a gap within the valence band is underestimated within the LDA, and the flat bands in the vicinity of the Fermi level do not separate completely (see, e.g., figure 3 of reference [4]). This is also the case in our calculation, which we have carried out for the experimental monoclinic structure as specified in reference [24]. The change from rutile to monoclinic structure gives rise to a broadening of the O 2p and V 3d bands by ~ 0.2 eV and to more pronounced splitting in the V 3d states of t_{2g} symmetry. In reference [25] it was shown that the inclusion of electron–phonon interaction (in the periodic shell model, based on the results of a discrete-variational X_α cluster calculation) leads to the opening of the band gap. According to our calculation, the distortion of the nested bands due to the displacement of the atoms in the doubled-cell monoclinic structure gives rise to only small changes in the partial DOS, as compared to the rutile structure. Technically, the calculation deals with two inequivalent oxygen species and three inequivalent types of lattice-packing empty spheres of different sizes, making a total of 24 sites. Our calculated total DOS for the monoclinic structure is shown in figure 1, lowest panel, and some partial DOS are shown in figure 2. For comparison with the XES,
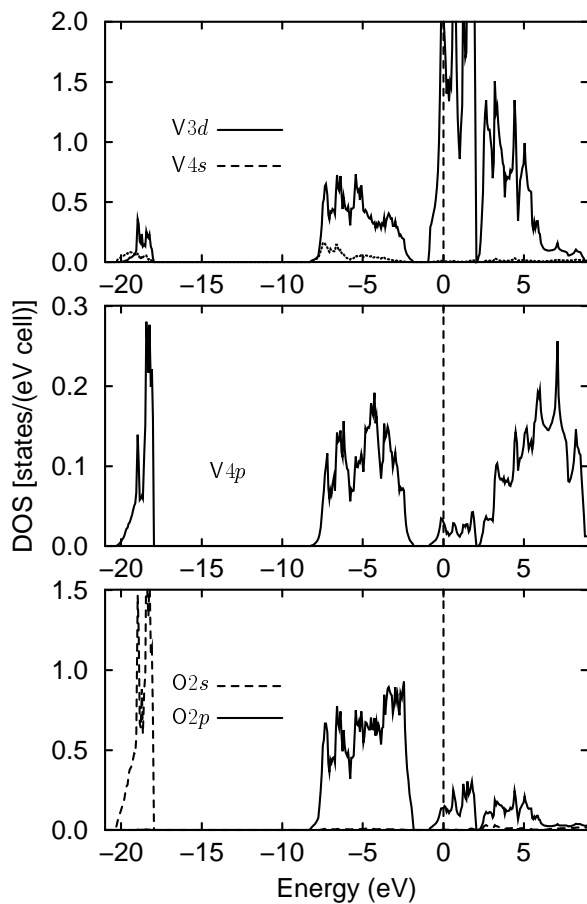
Figure 2. The partial density-of-states distribution in the monoclinic structure of VO$_2$.

we did not distinguish the data for the two oxygen species, and we show the averaged O 2s and O 2p DOS over all sites in figure 2, lowest panel. The densities of states are plotted for the $16 \times 16 \times 16$ mesh over the Brillouin zone.

Table 1. XPS binding energies and widths of the core levels (bands) of VO$_2$.

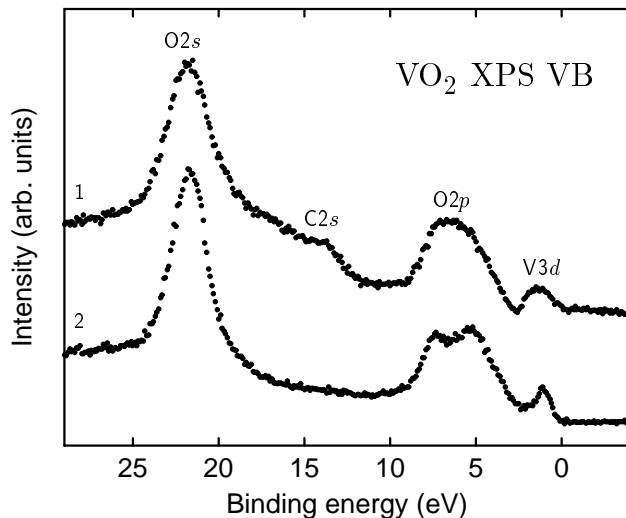| Core level (band)	Binding energy (eV)	FWHM (eV)
V 2s	630.02	6.10
O 1s	529.75	1.30
V 2p$_{1/2}$	523.48	2.56
V 2p$_{3/2}$	515.95	2.04
V 3s	68.95	4.54
V 3p	40.53	4.24
O 2s	21.73	2.5
O 2p	5.34; 7.24	
V 3d	1.03	

Figure 3. XPS VB spectra of uncleaved (1) and cleaved (2) surfaces of VO_2 single crystal.

3.2. X-ray photoelectron spectra

The intensity distribution of the VB XPS spectra reflects the total DOS of the VB, up to the deviations due to different atomic photoionization cross-sections. The results of the XPS measurements on single-crystal VO_2 are shown in figure 3 and in table 1.

The spectral measurements on the uncleaved crystal show a large contamination with carbon. This leads to a smearing of the fine structure over the entire valence band, a broadening of the subbands and the appearance of an additional subband at around 12–14 eV which we attribute to transitions from C 2s states.

In the XPS spectra of the cleaved VO_2 crystal, a distinct narrow peak is observed at around 1 eV below the Fermi level, which, according to the results of our band-structure calculations (see figure 2), has V 3d character. The FWHM of this peak is about 1 eV which is less than the value obtained in references [8–11].

The next subband has a two-peak structure at 3–9 eV below the Fermi level, which is mainly due to the O 2p states (cf. figure 2). Another reason for reaching this conclusion is that the energy difference between the centre of gravity of this band and the next one (located at 22 eV) is about 15 eV, which is in good agreement with the energy separation between O 2p and O 2s bands found in all vanadium oxides [26]. However, since the O 2p and V 3d atomic photoionization cross-sections for Al Kα excitation [27] have a ratio of about 1:2, one may expect some contribution of V 3d states in this band. This is also confirmed by our band-structure calculation and by the results from the V Lα emission measurements (see below). We point out, however, that the XPS and the ultraviolet photoelectron spectra (UPS) of VO_2 given in references [8–13] are at variance as regards the energy resolution and the intensity ratio of the two peaks. The peaks are well resolved in our measurements, and both their energy separation and the intensity ratio are in good agreement with the results of our band-structure calculations.

According to reference [28], charge-transfer satellites are found in the UPS of ScF_3, TiO_2 and V_2O_5 in the region from 11 to 17 eV below the top of the valence band. From the resonant photoemission measurements it was concluded that the charge-transfer-type configuration manifests itself in such a way as to form a valence state in the ground state in

addition to the originally filled 2p-state ligand. On the basis of this experimental evidence, cluster calculations of the valence photoemission and Bremsstrahlung isochromat spectra of VO$_2$ were performed in reference [6], and it was concluded that VO$_2$ belongs to the group of charge-transfer insulators. However, we point out that our XPS measurements on the uncleaved and cleaved VO$_2$ single crystal (figure 3) strongly suggest that the appearance of this structure (14–15 eV below the Fermi level) is connected with carbon contamination and that its origin is C 2s states. A similar problem was discussed in reference [29] in connection with the analysis of UPS spectra of superconducting cuprates. There, it was concluded that the satellites with binding energies of about 10 eV are genetically connected with contaminations with light elements and disappear after cleaning. Therefore we have found a clear indication that the structure in question is not an intrinsic feature of the electronic structure of pure VO$_2$ and cannot be considered as evidence of correlation effects in VO$_2$.
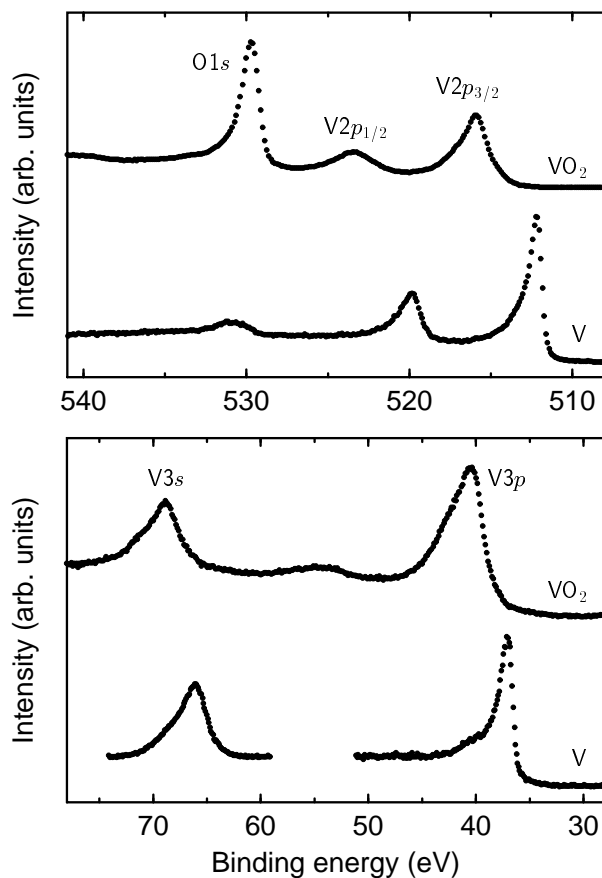

Figure 4. XPS O 1s, V 2p$_{3/2,1/2}$ (upper panel) and V 3s, V 3p (lower panel) core-level spectra of VO$_2$ and the metal V.

The XPS core-level spectra of VO$_2$ are shown in figure 4. The energy positions of the O 1s, V 2p and V 3p spectra of VO$_2$ are close to those of reference [9], but the FWHMs of the lines in these spectra (see table 1) are much smaller than those found in references [8, 9]. The line-shapes are clearly asymmetric due to a structure seen on the high-binding-energy

side. In the case of 2p and 3p levels this may be related to np^5d^1 multiplets, as was shown in reference [10] for the V 3p spectrum. It should be noted, however, that in our measurements the V 3p line-shape is somewhat different from that obtained in reference [10]. In the case of the V 3s level, the additional structure may be due to the exchange interaction of a (spin-up or spin-down) 3s electron left in the final state with the (V 3d) electrons in the valence band [30].

In figure 4, the V 2p, V 3s and V 3p XPS core-level spectra of VO_2 are compared with those of pure vanadium metal. Evidently, there is a chemical shift of the core-level spectra of VO_2 with respect to that of pure metal not only for the V 2p XPS line, but also for the V 3s and V 3p XPS lines. The fact that the formal charge of the vanadium atom affects V 3s and V 3p lines in a uniform way can be used as the basis of an estimation of the oxidation state of the V atom in compounds. Recently, the same conclusion was reached for the Mn 3s XPS spectra of manganese complexes in reference [31].

Earlier, we showed that the analysis of the 3s XPS spectra can be used to draw conclusions about the electronic structure of 3d-metal oxides [32]. It has been found that the 3s XPS spectra of NiO have a very complicated fine structure due to charge-transfer processes. In this case, an electron may be transferred from the ligand to a metal 3d level after the emission process, and both states, the screened and unscreened one, are visible in the 3s spectrum. The simpler fine structure of the V 3s XPS spectrum in VO_2 can be considered as evidence for negligible charge transfer, again indicating that the electronic structure of this compound is more bandlike than correlated.

3.3. X-ray emission spectra

X-ray emission valence spectra result from electron transitions between the valence band and a core hole. Since the wave function of a core electron is strongly localized and its angular momentum symmetry is well defined, these spectra reflect the site-projected and symmetry-restricted (in accordance with the dipole selection rules) partial DOS. In the case of VO_2, we have investigated V Lα (the $3d4s \rightarrow 2p_{3/2}$ transition), VKβ_5 (the $4p \rightarrow 1s$ transition) and O Kα emission spectra (the $2p \rightarrow 1s$ transition) which reflect the distribution of V 3d4s, V 4p and O 2p partial DOS. By means of XPS we can measure the binding energies of the V 2p and the O 1s core levels, so we can determine the position of the Fermi level in the x-ray emission spectra.

The O Kα and V Lα spectra, adjusted in such a way as to have a common energy scale with the x-ray photoemission spectrum, are shown in figure 5. The V Kβ_5 spectrum is positioned with respect to XPS by matching the position of the peak which results from the hybridization with O 2s states. In the same figure, the partial DOS as calculated for the monoclinic phase and broadened with an energy-dependent Lorentzian linewidth according to reference [33] are shown. The calculated and broadened partial DOS have been rigidly shifted with respect to the Fermi energy (arbitrarily, but by the same amount for all of the spectra) to account for a systematic error in the energy matching of the measured spectra and calculated DOS due to, e.g., the absence of the band gap in the calculation.

As can be seen, the main maximum of the O Kα spectrum (O 2p states) is placed near the top of the valence band, which is quite common for oxides, and is essentially non-bonding. A corresponding feature is also seen in the XPS, but merely as a shoulder at 4 eV, due to a smaller value of the O 2p photoionization cross section as compared to that for V 3d [27]. The XPS VB fine structure with two peaks at 5.4 and 7.5 eV reveals the O 2p–V 3d bonding band, which overlaps in energy with the maximum of the V Lα spectrum and with a high-binding-energy hump of the O Kα spectrum.
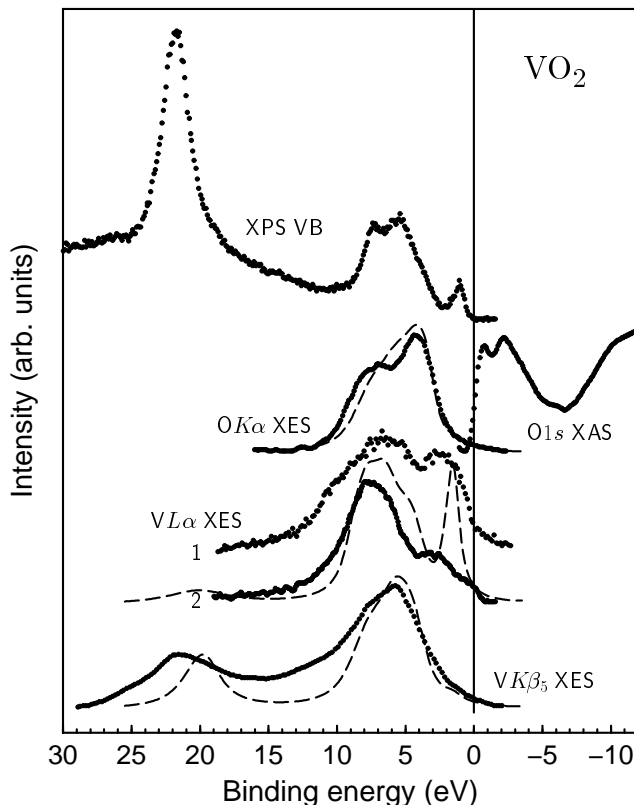
Figure 5. Dots: the comparison of the XPS VB, XES (O Kα (fluorescent excitation at $E = 530.8$ eV), V Lα (curve 1 corresponds to electron excitation at $E = 4.4$ keV, curve 2 to fluorescent excitation at $E = 519.0$ eV), V Kβ_5 (fluorescent excitation at $E = 15$ keV)) and XAS O 1s spectra of the VO$_2$ single crystal. Dashed lines: broadened partial O 2p, V 3d and V 4p (from top to bottom) DOS as calculated for monoclinic VO$_2$.

We have excited O Kα emission at two excitation energies ($E = 530.8$ and 532.2 eV) which correspond to the maxima of the O 1s x-ray absorption spectrum (XAS), but found only little difference. The V Lα emission spectrum has been obtained with both electron and photon excitation, which resulted in different intensity distributions (curves 1 and 2 in figure 5). With electron excitation at $E = 4.4$ keV (curve 1), we have simultaneous excitation of V Lα (3d4s $\rightarrow$ 2p$_{3/2}$) and V Lβ emissions (3d4s $\rightarrow$ 2p$_{1/2}$) which are separated by only 7.53 eV. Therefore there is an overlap of the high-energy subband of the V Lα XES with the main peak of the V Lβ emission spectrum. For an excitation energy $E = 519.0$ eV (curve 2), we selectively excite only V Lα. From these data one can conclude that there is a considerable admixture of V 3d states in the O 2p-like bands, so the maximum emission comes from the V 3d–O 2p hybridized band and not from an only slightly populated V 3d band. We find that the fine structure and energy position of the subbands of the V Lα emission spectrum are in reasonable agreement with the calculated V 3d partial DOS distribution given in figure 2.

The V Kβ_5 emission spectrum has two main subbands whose energy positions are very close to the O 2p and the O 2s bands due to V 4p–O 2p and V 4p–O 2s hybridization (see figure 2). The splitting of the main subband of the V Kβ_5 emission spectrum also follows

the calculated V 4p DOS distribution in this energy region. It is seen that the admixture of the V 4p states with the V 3d band is too small to be detected in the V Kβ_5 XES of VO_2. The disagreement by $\sim$2 eV between the spectra (XPS; V Kβ_5) and the calculated DOS as regards the position of the O 2s states is known in oxides. This is related to the fact that the hole relaxation, which effectively increases the binding energy of an electron leaving a comparatively localized state such as O 2s, is not taken into account in our band-structure calculations which describe the ground state but not excitations.

It should be mentioned that soft-x-ray fluorescence spectra of VO_2 (V Lα, β, O Kα XES) were also recently reported in reference [11] and are compared with an UPS spectrum (measured at $E = 501.1$ eV); however, no XPS measurements of the V 2p and the O 1s binding energies are included there. The O Kα XES of reference [11] does not show the two-peak structure found in our measurements.

3.4. Total-electron-yield spectra

O 1s XAS of VO_2 probes the O 2p unoccupied states. Such spectra, with good energy resolution, have been published earlier, by Abbate *et al* [34]. In order to compare the XES obtained on the same samples as were used in the XPS, we include in figure 5 our own O 1s spectrum obtained (for the monoclinic phase) in the sample drain-current mode. The Fermi level has been determined with the help of the XPS binding energy of the O 1s level given in table 1. The O 1s spectrum was measured over a rather restricted energy range, so we can only compare the spectra in the vicinity of the Fermi level.

The fine structure of the O 1s spectrum is in agreement with the shape of the O 2p conduction band in our electronic structure calculations (figure 2). In the high-temperature rutile phase, the calculated conduction band exhibits a pronounced two-peak structure, also discussed in reference [34]. In the low-temperature monoclinic phase, a further splitting of the conduction band is seen from the calculations, in agreement with a more pronounced structure in the O 1s spectrum of reference [34].

4. Conclusion

The results of measurements of high-resolution x-ray photoelectron spectra, V Lα, V Kβ_5 and O Kα x-ray emission spectra (obtained by using both electron and x-ray excitation) and O 1s absorption spectra of a VO_2 single crystal are presented. They are compared with first-principles LMTO band-structure calculations of VO_2 in the monoclinic and tetragonal rutile phases. It is concluded that the electronic structure of VO_2 is more bandlike than correlated.

References

[1] Adler D 1968 *Solid State Physics* vol 21 (New York: Academic) p 1
[2] Goodenough J B 1960 *Phys. Rev.* **117** 1442
[3] Gupta M, Freeman A J and Ellis D E 1977 *Phys. Rev.* B **16** 3338
[4] Wentzcovitch R M, Schulz W W and Allen P B 1994 *Phys. Rev. Lett.* **72** 3389
[5] Sommers C, de Groot R, Kaplan D and Zylbersztein A 1975 *J. Physique Lett.* **36** L157
[6] Uozumi T, Okada K and Kotani A 1993 *J. Phys. Soc. Japan* **62** 2595
[7] Zaanen J, Sawatzky G A and Allen J W 1985 *Phys. Rev. Lett.* **55** 418
[8] Blaauw C, Leenhouts F, van der Woude F and Sawatzky G A 1975 *J. Phys. C: Solid State Phys.* **8** 459
[9] Sawatzky G A and Post D 1979 *Phys. Rev.* B **20** 1546
[10] Shin S, Suga S, Taniguchi M, Fujisawa F, Kanzaki H, Fujimori A, Daimon H, Ueda Y, Kosuge K and Kachi S 1990 *Phys. Rev.* B **41** 4993
[11] Shin S, Agui A, Watanabe M, Fujisawa M, Tezuka Y and Ishii T 1995 *ISSP Technical Report* Series A, No 3038
[12] Goering E, Schramme M, Müller O, Barth R, Paulin H, Klemm M, den Boer M L and Horn S 1997 *Phys. Rev.* B **55** 4225
[13] Goering E, Schramme M, Müller O, Paulin H, Klemm M, den Boer M L and Horn S 1997 *Physica* B **230–232** 996
[14] Dolgih V E, Cherkashenko V M, Kurmaev E Z, Goganov D A, Ovchinnikov E K and Yarmoshenko Yu M 1984 *Nucl. Instrum. Methods Phys. Res.* **224** 117
[15] Pfugler J and Gurtler P 1993 *Nucl. Instrum. Methods Phys. Res.* A **287** 628
[16] Nordgren J, Bray G, Gramm S, Nyholm R, Rubensson J E and Wassdahl N 1989 *Rev. Sci. Instrum.* **60** 1690
[17] Andersen O K and Jepsen O 1984 *Phys. Rev. Lett.* **53** 2571
Andersen O K, Pawlowska Z and Jepsen O 1986 *Phys. Rev.* B **34** 5253
[18] von Barth U and Hedin L 1972 *J. Phys. C: Solid State Phys.* **5** 1629
[19] Langreth D C and Mehl M J 1981 *Phys. Rev. Lett.* **47** 446
Langreth D C and Mehl M J 1983 *Phys. Rev.* B **28** 131
[20] McWhan D B, Marezio M, Remeika J P and Dernier P D 1974 *Phys. Rev.* B **10** 490
[21] Caruthers E, Kleinman L and Zhang H I 1973 *Phys. Rev.* B **7** 3753
[22] Nikolaev A V, Kostrubov Yu N and Andreev B N 1992 *Fiz. Tverd. Tela* **34** 3011 (Engl. Transl. *Sov. Phys.–Solid State* **34** 1614)
[23] Caruthers E and Kleinman L 1973 *Phys. Rev.* B **7** 3760
[24] Andersen G 1956 *Acta Chem. Scand.* **10** 623
[25] Nakatsugawa H and Iguchi E 1997 *Phys. Rev.* B **55** 2157
[26] Cherkashenko V M, Kurmaev E Z, Fotiev A A and Volkov V L 1975 *Sov. Phys.–Solid State* **17** 167
[27] Yeh J J and Lindau I 1985 *At. Data Nucl. Data Tables* **32** 1
[28] Shin S, Tezuka Y, Ishii T and Ueda Y 1993 *Solid State Commun.* **87** 1051
[29] Takahashi T, Maeda F, Katayama-Yoshida H, Okabe Y, Suzuki T, Fujimori A, Hosoya S, Shamoto S and Sato M 1988 *Phys. Rev.* B **37** 9788
[30] van Vleck J H 1934 *Phys. Rev.* **15** 405
[31] Fujiwara M, Matsushita T and Ikeda S 1995 *J. Electron Spectrosc. Relat. Phenom.* **74** 201
[32] Uhlenbrock St, Bartkowski St, Postnikov A V, Mayer B, Neumann M, Galakhov V R, Finkelstein L D, Kurmaev E Z and Leonyuk L I 1998 unpublished
[33] Blokhin M A and Sachenko V P 1960 *Izv. Akad. Nauk SSSR, Ser. Fiz.* **24** 397
[34] Abbate M, Pen H, de Groot F M F, Fuggle J C, Ma Y J, Chen C T, Sette F, Fujimori A, Ueda Y and Kosuge K 1991 *Phys. Rev.* B **43** 7263